13th International Conference on
Structural Health Monitoring of Intelligent Infrastructure
DOI: 10.3217/978-3-99161-057-1-132

Field test on tunnel indirect damage identification from moving train response

Qi Li[1, 2], Xiongyao Xie[1, 2], Kun Zeng[1, 2]
[1]Department of Geotechnical Engineering, School of Civil Engineering, Tongji University, Shanghai 200092, People's Republic of China
[2]Key Laboratory of Geotechnical and Underground Engineering of Ministry of Education, School of Civil Engineering, Tongji University, Shanghai 200092, People's Republic of China
email: 2310026@tongji.edu.cn, xiexiongyao@tongji.edu.cn, zengkun_tj@tongji.edu.cn

ABSTRACT: To explore the potential application of the tunnel damage identification method based on train acceleration, a three-axis accelerometer was installed on a metro train carriage to collect acceleration signals. The original signals are segmented and aligned according to the stations, with data analyzed in terms of station sections. Next, the probability density distribution, fast Fourier transform spectrum, and one-third octave spectrum of the signal are calculated. A time-frequency domain fast analysis software for acceleration data is then developed. By comparing changes in time-frequency domain features, the anomalous section of the tunnel is identified. The results confirm that the tunnel damage identification method based on train acceleration is applicable for real-world metro tunnels.

KEY WORDS: Field test; Probability density distribution; Fast Fourier transform; One-third octave.

1 INTRODUCTION

With the rapid pace of urbanization, metro systems are playing an increasingly vital role in alleviating urban traffic congestion [1]. As a critical support infrastructure for metro trains, metro tunnels can experience issues such as settlement, water leakage, and lining cracks during their operational period [2]. These problems can arise from the combined effects of geological conditions, material aging, dynamic loads from trains, and nearby construction activities, all of which can compromise the structural integrity of the tunnels [3]-[4]. Therefore, monitoring the health condition of metro tunnels and performing timely maintenance are crucial for ensuring the safe and efficient operation of the metro system [5].

Li [6] proposed a method that involves installing acceleration sensors on metro trains to identify tunnel damage or anomalies by analyzing changes in train acceleration. The feasibility of this approach was demonstrated theoretically. This method offers advantages such as high efficiency and low cost, providing a novel approach to metro tunnel health monitoring. Following this, damage indicators based on wavelet packet energy change rates [6], spectral kurtosis change rates [6], and relative entropy of wavelet packet energy [7] were introduced for analyzing train acceleration signals to identify tunnel anomalies. Deep learning techniques, including convolutional variational autoencoders (CVAE) [7], convolutional neural networks (CNN) [8], and long short-term memory (LSTM) [8] networks, have been applied to classify tunnel damage types, with their performance validated through model tests. Compared to traditional damage indicators, deep learning methods effectively reduce the interference from noise and data inconsistencies. Although the feasibility of the tunnel damage identification method based on train acceleration has been theoretically and experimentally verified, real-world acceleration data from metro trains have yet to be collected to assess the feasibility of the method in field conditions.

In this study, a three-axis accelerometer was installed on a metro train carriage to collect the train acceleration. The time-frequency domain features of the acceleration signals are then calculated. By analyzing the changes in these features, the anomalous section of the tunnel is identified. The results confirm that the tunnel damage identification method based on train acceleration is feasible for real-world applications.

2 FIELD TEST

In this study, a field test was conducted on a complete metro line in a certain city, which includes two tunnels on the up and down lines, with a total of 19 stations. A wireless three-axis accelerometer, with a measurement range of 2g and a sampling frequency of 4000Hz, was installed under the seat in the middle of the train carriage to collect the train acceleration. The test, as outlined in Table 1, was conducted in three phases from April 16 to September 20, 2021, spanning a total of 24 days. For each test day, a set of acceleration data was recorded from the starting station to the terminal station, with separate data sets collected for both the up and down line tunnels.

Table 1. Test dates.

Phase	Dates
Phase 1	April 16 - April 28
Phase 2	May 12 - May 21
Phase 3	September 20

3 TEST DATA ANALYSIS

3.1 Original data

The original signal is segmented and aligned based on the 19 stations, dividing the line into 18 station sections for sectional data analysis. Taking a specific section as an example, the acceleration signal is shown in Figure 1. In this figure, the X direction represents the forward direction of the train, while the Z direction is perpendicular to the ground of the carriage. The acceleration in the X direction shows a clear ascending or

DOI: 10.3217/978-3-99161-057-1-132

descending trend due to changes in train speed, whereas the acceleration in the Y and Z directions exhibits similar patterns of variation.

In this study, the Z direction is selected to analyze the changes in train acceleration. The acceleration in the Z direction for 18 sections is shown in Figure 2. The number above each curve corresponds to the section's serial number. Due to variations in tunnel length, geological conditions, and track irregularities across the sections, the time-domain waveforms of acceleration exhibit distinct differences.

The acceleration in the Z direction for 6 days in the same section is shown in Figure 3. The numbers above the curves in the figure represent the corresponding dates, with April 19 recorded as 4.19, and so on. Since the train's speed and the mass of the carriage vary slightly each day, the acceleration values in the same section show some differences in amplitude.

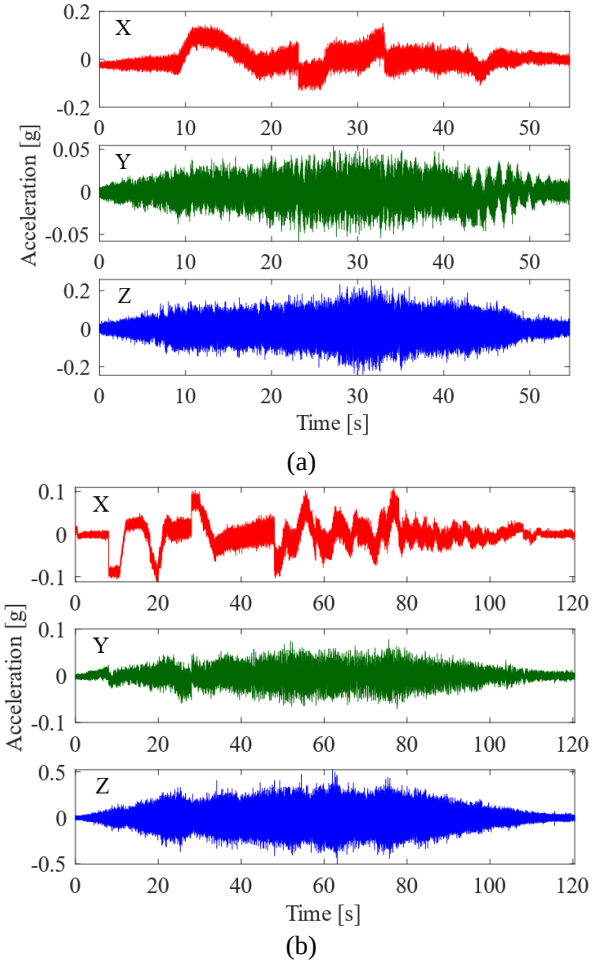

(a)

(b)

Figure 1. Acceleration signals in the X, Y, and Z directions: (a) Up line; (b) Down line.

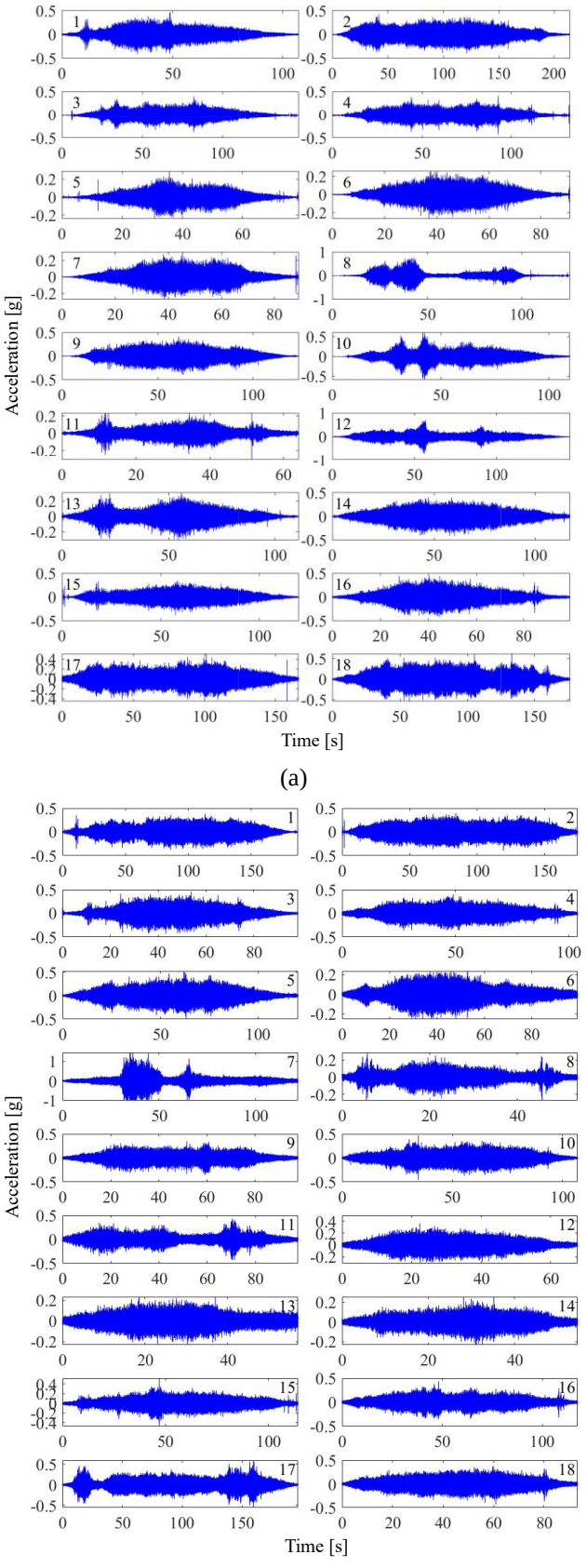

(a)

(b)

Figure 2. Acceleration signals in different sections: (a) Up line; (b) Down line.

DOI: 10.3217/978-3-99161-057-1-132

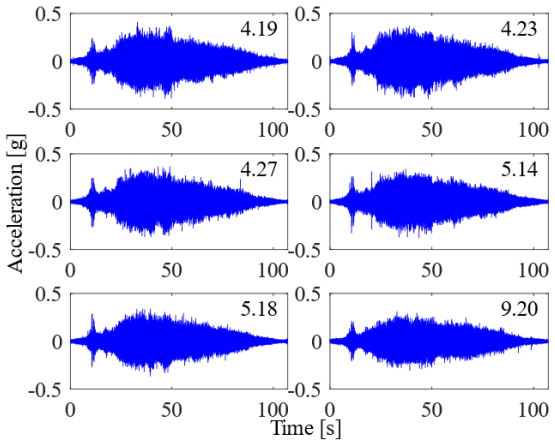

(a)

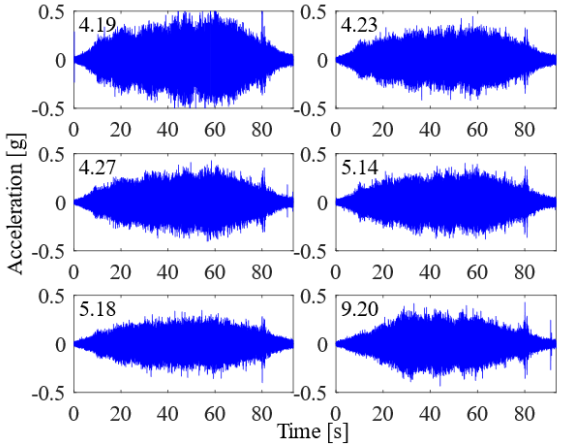

(b)

Figure 3. Acceleration signals on different dates: (a) The 1st section of the up line; (b) The 18th section of the down line.

3.2 *Probability density distribution*

The probability density distribution curve of the acceleration signals for 6 days within the same section is shown in Figure 4, with the FIT curve representing the normal distribution fit. The mean acceleration values within the same section are similar, while there are differences in variance.

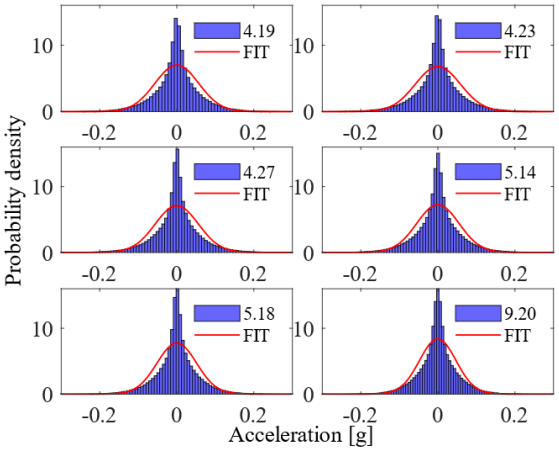

(a)

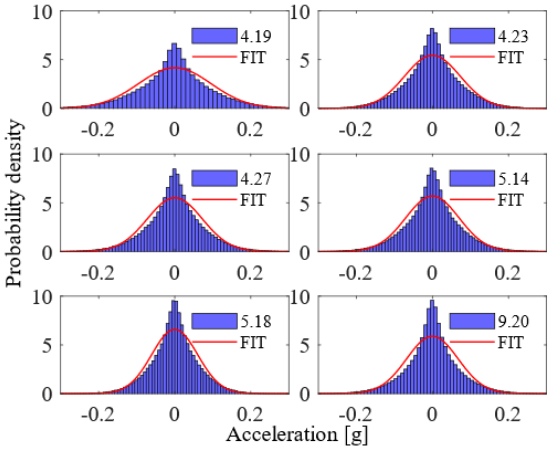

(b)

Figure 4. Probability density distribution curves of acceleration signals on different dates: (a) The 1st section of the up line; (b) The 18th section of the down line.

3.3 *Fast Fourier transform*

The acceleration signals from 24 days are analyzed using fast Fourier transform (FFT), converting the time-domain signals into the frequency domain. As shown in Figure 5, the blue curve represents the average of the FFT results from all the signals. The signal energy is concentrated between 200 and 800 Hz, with peaks around 450 Hz and 700 Hz.

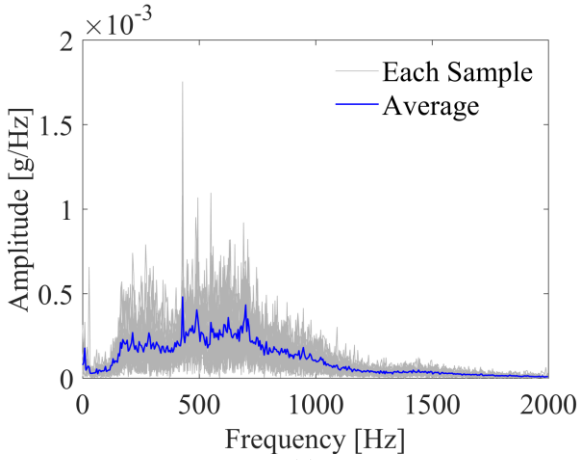

(a)

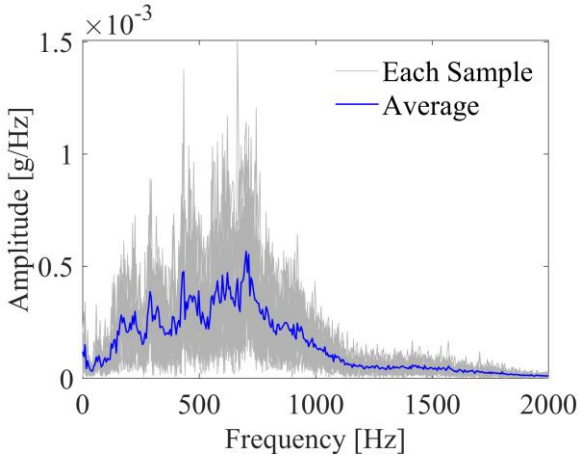

(b)

DOI: 10.3217/978-3-99161-057-1-132

Figure 5. Fast Fourier transform spectrum of acceleration signals: (a) The 1st section of the up line; (b) The 18th section of the down line.

3.4 One-third octave

Figure 6 shows the one-third octave spectrum of the acceleration signals over 24 days, illustrating the distribution of signal energy across different frequency bands. The blue curve in the figure represents the average energy of all the signals. Similar to the FFT spectrum, the signal energy exhibits a peak around 700 Hz.

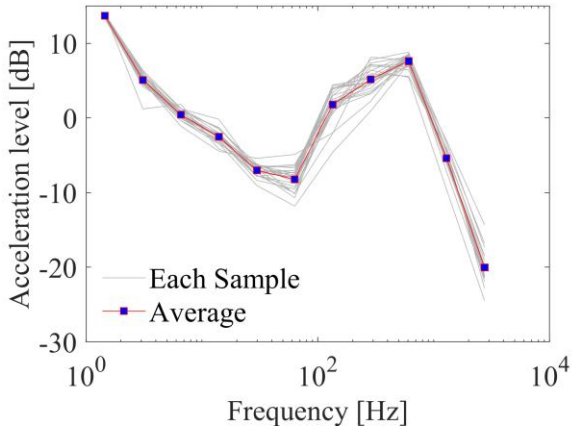

(a)

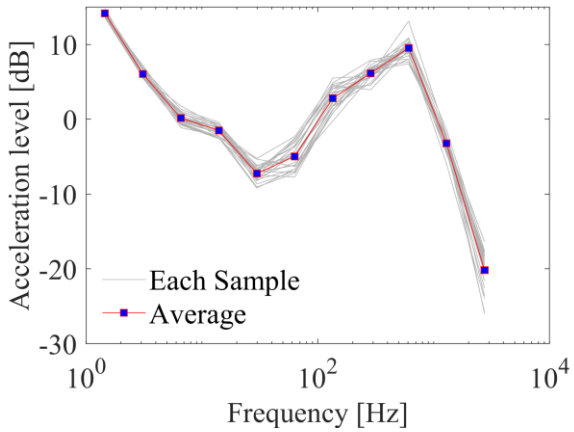

(b)

Figure 6. One-third octave spectrum of acceleration signals: (a) The 1st section of the up line; (b) The 18th section of the down line.

3.5 Time-frequency domain fast analysis software

As shown in Figure 7, a time-frequency domain fast analysis software for acceleration data is developed using MATLAB App Designer. First, click “Data loading” to read the train acceleration signal from the input “File name”. Next, select or enter the line direction (Left, i.e., Down, or Right, i.e., Up), section number, date, and acceleration direction (X, Y, or Z). Finally, by clicking the “Time domain data”, “Probability density curve”, “Fast Fourier transform”, and “One-third octave” buttons, users can quickly compute and visualize the time-frequency domain features of the signal, facilitating further comparative analysis.

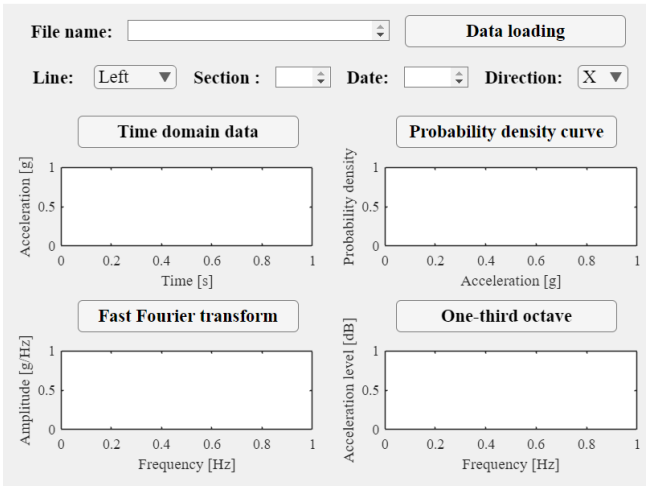

(a)

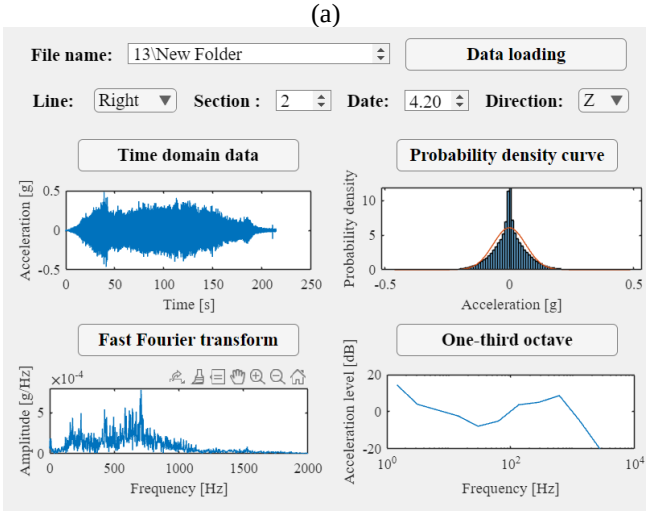

(b)

Figure 7. Time-frequency domain fast analysis software for acceleration data: (a) Software interface; (b) Visualization of analysis results.

4 DATA ANALYSIS OF ANOMALOUS SECTION

4.1 Time domain analysis

As shown in Figure 8 and Figure 9, during the data analysis, it is observed that the acceleration signals in the 2nd section of the up line and the 17th section of the down line show significant changes over time. These two sections correspond to the left and right tunnels of the same station segment. Comparing this with the section's operation and maintenance records reveals that, during the field test, the tunnel linings of this station segment experienced excessive uplift, which altered the tunnel's stiffness and boundary conditions. This change is reflected in noticeable differences in the train's vibration signal waveforms. Additionally, on the test day, September 20, which was a rainy day, the tunnel's boundary conditions were further modified, resulting in a significant increase in the train's acceleration amplitude.

DOI: 10.3217/978-3-99161-057-1-132

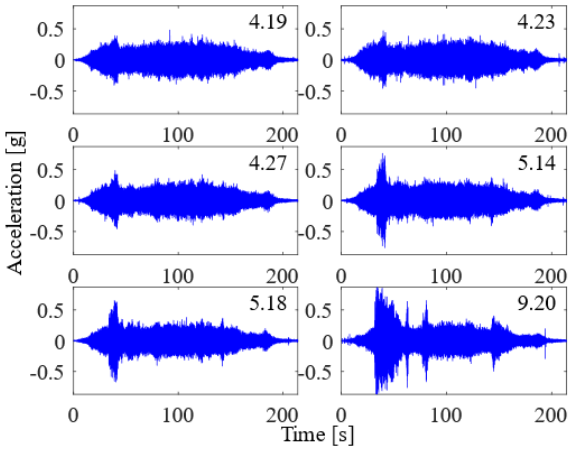

(a)

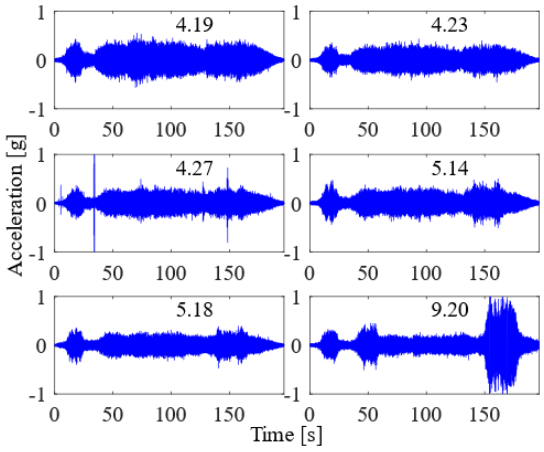

(b)

Figure 8. Acceleration signals of the anomalous section: (a) The 2nd section of the up line; (b) The 17th section of the down line.

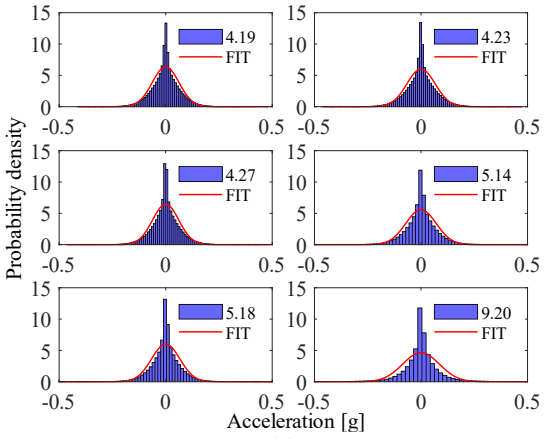

(a)

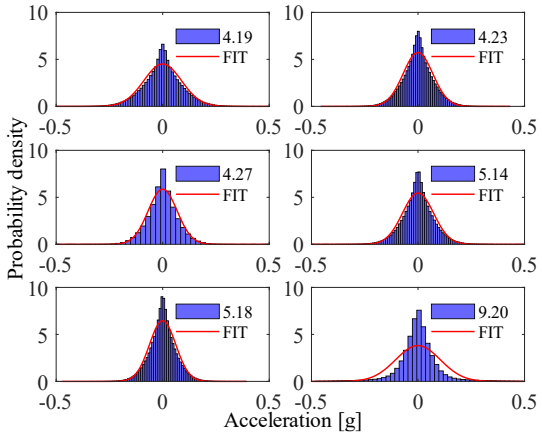

(b)

Figure 9. Probability density distribution curves of acceleration signals in the anomalous section: (a) The 2nd section of the up line; (b) The 17th section of the down line.

4.2 Frequency domain analysis

Further analysis of the frequency domain features for the acceleration signals in the anomalous section, shown in Figure 10 and Figure 11, reveals an increase in energy around 700 Hz compared to the normal sections.

The discovery of the anomalous section validates the feasibility of tunnel damage identification method based on train acceleration for field applications. By analyzing the changes in the time-frequency domain features of the train's acceleration signals, tunnel anomalies can be indirectly identified.

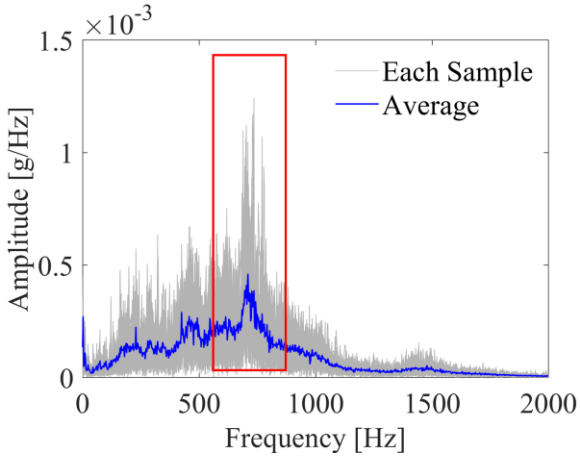

(a)

DOI: 10.3217/978-3-99161-057-1-132

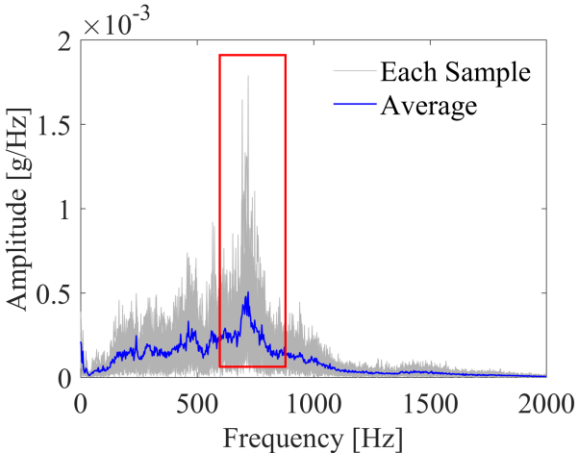

(b)

Figure 10. Fast Fourier transform spectrum of acceleration signals in the anomalous section: (a) The 2nd section of the up line; (b) The 17th section of the down line.

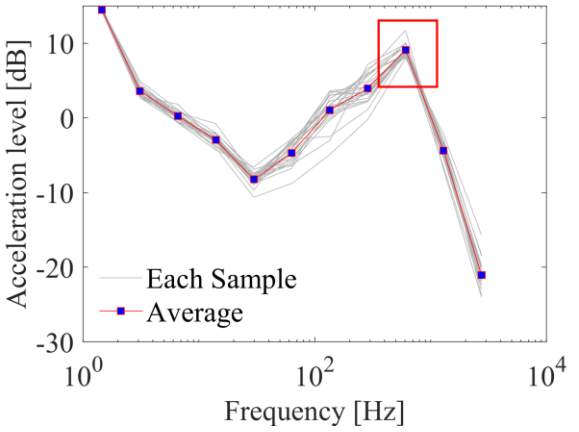

(a)

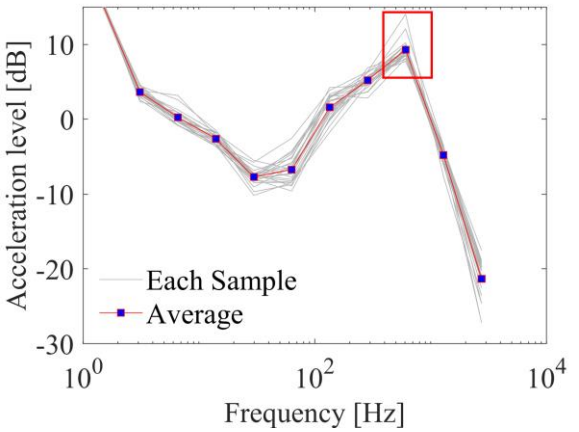

(b)

Figure 11. One-third octave spectrum of acceleration signals in the anomalous section: (a) The 2nd section of the up line; (b) The 17th section of the down line.

5 CONCLUSIONS

In this study, a three-axis accelerometer was installed on the train carriage to collect acceleration signals throughout the entire journey. The time-frequency domain features of the signals are analyzed. The main conclusions of this study are as follows:

1) The acceleration in the direction of the train's motion shows distinct ascending or descending segments due to changes in train speed. The acceleration in the two directions perpendicular to the train's motion exhibits a similar trend.

2) The train acceleration signals in normal sections on different dates show slight differences in amplitude due to variations in train speed and carriage mass. In contrast, the train acceleration signals in anomalous sections on different dates exhibit significant differences in waveform, caused by changes in the tunnel's stiffness and boundary conditions, with more substantial fluctuations in signal amplitude.

3) By calculating the probability density distribution, fast Fourier transform spectrum, and one-third octave spectrum of the acceleration signals, changes in the time-frequency domain features can reveal anomalous sections of the tunnel. This analysis validates the feasibility of tunnel damage identification method based on train acceleration in real-world applications.

Future work will involve selecting additional metro tunnels, installing sensors on trains to collect field data, and building a comprehensive dataset. Machine learning or deep learning techniques will then be applied to further identify tunnel anomalies.

ACKNOWLEDGMENTS

This work was supported by the National Natural Science Foundation of China (grant no. 52038008).

REFERENCES

[1] Zhou, C., Qin, W., Luo, H., Yu, Q., Fan, B., & Zheng, Q. (2024). Digital twin for smart metro service platform: Evaluating long-term tunnel structural performance. *Automation in Construction*, 167, 105713. https://doi.org/10.1016/j.autcon.2024.105713.

[2] Zheng, A., Qi, S., Cheng, Y., Wu, D., & Zhu, J. (2024). Efficient Detection of Apparent Defects in Subway Tunnel Linings Based on Deep Learning Methods. *Applied Sciences*, 14(17), 7824. https://doi.org/10.3390/app14177824.

[3] Yang, H., Wang, L., Pan, Y., & Chen, J. J. (2025). A Teacher-Student Framework Leveraging Large Vision Model for Data Pre-Annotation and YOLO for Tunnel Lining Multiple Defects Instance Segmentation. *Journal of Industrial Information Integration*, 100790. https://doi.org/10.1016/j.jii.2025.100790.

[4] Lin, W., Li, P., Xie, X., Cao, Y., & Zhang, Y. (2023). A Novel Back-Analysis Approach for the External Loads on Shield Tunnel Lining in Service Based on Monitored Deformation. *Structural Control and Health Monitoring*, 2023(1), 8128701. https://doi.org/10.1155/2023/8128701.

[5] Chen, X., Zhang, Q., Liu, R., Wang, X., & He, W. (2023). Maintenance strategies and life-cycle cost analysis of inspection robots in metro tunnels. *Tunnelling and Underground Space Technology*, 140, 105270. https://doi.org/10.1016/j.tust.2023.105270.

[6] Li, H., Xie, X., Zhang, Y., & Wang, Q. (2021). Theoretical, numerical, and experimental study on the identification of subway tunnel structural damage based on the moving train dynamic response. *Sensors*, 21(21), 7197. https://doi.org/10.3390/s21217197.

[7] Zhang, Y., Xie, X., Li, H., & Zhou, B. (2022). An unsupervised tunnel damage identification method based on convolutional variational auto-encoder and wavelet packet analysis. *Sensors*, 22(6), 2412. https://doi.org/10.3390/s22062412.

[8] Zhang, Y., Xie, X., Li, H., Zhou, B., Wang, Q., & Shahrour, I. (2022). Subway tunnel damage detection based on in-service train dynamic response, variational mode decomposition, convolutional neural networks and long short-term memory. *Automation in Construction*, 139, 104293. https://doi.org/10.1016/j.autcon.2022.104293.